Physics of the Solid State, Vol. 46, No. 3, 2004, pp. 395–410. Translated from Fizika Tverdogo Tela, Vol. 46, No. 3, 2004, pp. 385–400.

REVIEWS

New Type of Domain Walls: Domain Walls Caused by Frustrations in Multilayer Magnetic Nanostructures

A. I. Morosov and A. S. Sigov

Moscow State Institute of Radioengineering, Electronics, and Automation (Technical University), pr. Vernadskogo 78, Moscow, 119454 Russia

e-mail: mor-alexandr@yandex.ru

Received May 26, 2003

Abstract—Roughness of the interfaces between layers in a multilayer magnetic structure causes frustration of the exchange interaction between spins. Under certain conditions, frustration brings about the formation of domain walls (DWs) of a new type, whose parameters are determined by the competition between different exchange interactions rather than between the exchange and anisotropy energies as is the case with conventional DWs. Such DWs are much sharper than conventional DWs. The conditions under which micro- (nano-) domains arise are considered, and magnetic phase diagrams for ferromagnet–nonmagnetic metal–ferromagnet and ferromagnet–antiferromagnet nanostructures are discussed. © *2004 MAIK "Nauka/Interperiodica".*

1. INTRODUCTION

Multilayer magnetic structures several nanometers thick have been attracting considerable research attention since the discovery of giant magnetoresistance (GMR) [1], which immediately found wide practical application. This effect is used, in particular, in reading heads for gigabyte hard disks in personal computers. Such heads made it possible to increase the recording density and, hence, the memory capacity of hard disks. Multilayer magnetic structures are widely used as magnetic-field sensors and are still finding new areas of application. They offer promise as a basis for nonvolatile magnetic random-access memory (MRAM), which could be expected to take the place of both hard disks and semiconductor-based RAM.

Multilayer magnetic nanostructures are also of considerable interest from the fundamental point of view. In the case of such thin layers (ranging in thickness from several nanometers to several tens of nanometers), the effect of interfaces is very significant and the properties of thin layers can differ radically from those of the corresponding bulk materials. Furthermore, the condition of the interfaces has been found to dictate the physical and, in particular, magnetic properties of the layers. The present review is devoted to this topic.

The review is organized as follows. In Section 2, we discuss frustration in multilayer magnetic structures. Section 3 deals with domain walls (DWs) due to frustration and with a phase diagram for the ferromagnet–nonmagnetic metal–ferromagnet three-layered structure. The ferromagnet–antiferromagnet two-layer system is considered in Section 4, and the ferromagnet–antiferromagnet–ferromagnet three-layered system is treated in Section 5. Finally, in Section 6, the main conclusions are drawn and lines of further investigations are proposed.

2. FRUSTRATION IN MULTILAYER MAGNETIC STRUCTURES

2.1. Giant Magnetoresistance

Let us briefly consider giant magnetoresistance on the example of a ferromagnet–nonmagnetic metal–ferromagnet three-layer metallic system with ideally smooth interfaces (Fig. 1). The exchange coupling between the ferromagnetic (FM) layers is effected through a paramagnetic spacer layer of thickness d via the Ruderman–Kittel–Kasuya–Yosida (RKKY) interaction. The exchange integral $J_\perp(d)$ in the case of free electrons has the form [2]

$$J_\perp(d) = J_0 \frac{\sin(2k_F d)}{(2k_F d)^2}, \quad (1)$$

where J_0 is a constant and k_F is the Fermi wave vector of conduction electrons.

Expression (1) takes no account of the specific shape of the Fermi surface of the nonmagnetic spacer

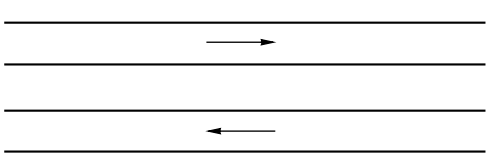

Fig. 1. Ferromagnet–nonmagnetic metal–ferromagnet three-layered system (schematic).

1063-7834/04/4603-0395$26.00 © 2004 MAIK "Nauka/Interperiodica"

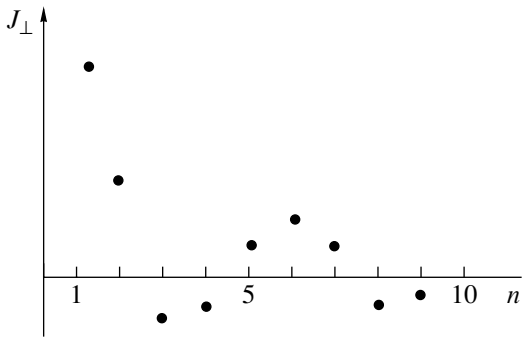

Fig. 2. Exchange integral of interlayer interaction as a function of the number of atomic planes in the nonmagnetic spacer layer.

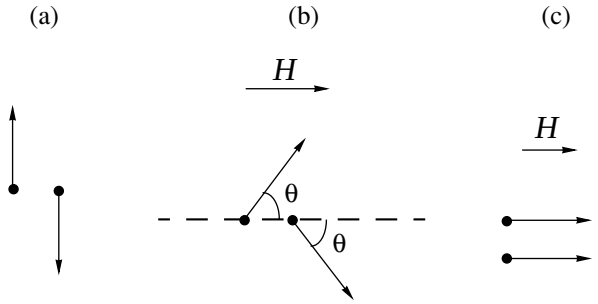

Fig. 3. Orientation of the magnetization vectors of FM layers corresponding to different ranges of values of the external magnetic field in the exchange approximation. (a) $H = 0$, (b) $H < H_{sat}$, and (c) $H > H_{sat}$.

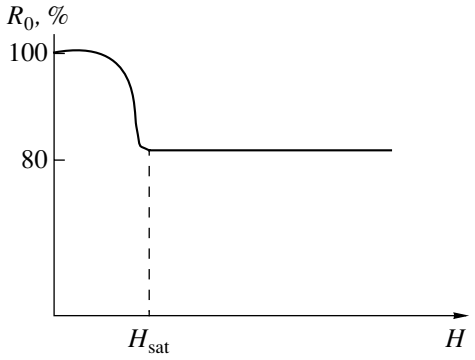

Fig. 4. Resistance of a magnetic multilayer structure as a function of external magnetic field.

and the size effects due to finite transverse dimensions of the layers. These effects have been considered in a large number of papers (see, e.g., [3–7]). The $J_\perp(d)$ dependence can also be strongly affected by the presence of several extremal cross-sectional dimensions of the complicated Fermi surface resulting in a superposition of spatial oscillations with different periods. However, the factors indicated above do not change the oscillatory character of the exchange coupling between the FM layers.

It should also be noted that the thickness d takes on discrete values, changing by one atomic layer. The dependence of $J_\perp$ on the number n of atomic layers is shown in Fig. 2.

It can be seen from Fig. 2 that $J_\perp$ is negative at certain values of n. Therefore, the interaction energy E_{int} between the FM layers

$$E_{int} = -J_\perp(\mathbf{M}_1, \mathbf{M}_2) \quad (2)$$

is minimal when the magnetizations $\mathbf{M}_1$ and $\mathbf{M}_2$ of the layers are antiparallel. It is this magnetization orientation that is realized in the absence of an external magnetic field. When a magnetic field is applied, the magnetization of each layer tends to be oriented along the magnetic field. Therefore, as the magnetic field is increased, the mutual orientation of the magnetizations changes from antiparallel to canted (Fig. 3) and then, as the saturation field H_{sat} is reached, the magnetizations become parallel. In the case where the two FM layers are identical, the magnetizations behave in the same way as the magnetizations of a mirror-symmetric antiferromagnet in an external magnetic field.

When the mutual orientation of adjacent FM layers of a three-layer structure (or of a multilayer structure consisting of alternating FM and nonmagnetic layers) changes from antiparallel to parallel, the resistance of the structure decreases by several percent or several tens of percent; that is, GMR takes place. The typical dependence of the resistance $R_0(H)$ on magnetic field is shown in Fig. 4.

Naturally, for the values of n at which $J_\perp > 0$, the magnetizations of layers are parallel to each other even in the absence of a magnetic field and GMR does not occur.

Here, we do not discuss the mechanisms of GMR and refer the reader to the recent review dedicated to this subject [8]. It should be noted that many simple explanations of GMR involve (explicitly or implicitly) the assumption that the mean free path of charge carriers is less than the layer thicknesses, which is not the case even at room temperature in the range of layer thicknesses in question in this review.

2.2. Frustration in a Three-Layered System with a Nonmagnetic Spacer Layer

The simple pattern of magnetic ordering considered above occurs in the case with ideally smooth interfaces between layers. In actuality, the layer interfaces are rough; i.e., the spacer is not uniform in thickness. In the case of crystalline layers (to which we will restrict our consideration), the roughness is due to atomic steps that arise on the interfaces and change the layer thickness by one monatomic layer (Fig. 5).

Let us consider how atomic steps affect the coupling between FM layers, which is the sum of pairwise RKKY interactions between atomic spins belonging to different layers. For this purpose, we should determine the region that contributes to the molecular field exerted by one layer on the atomic spin of the other layer.

A simple analysis shows that this region lies opposite the atom and that its size is typically of the order of the thickness of the nonmagnetic spacer d (Fig. 5). In other words, the thickness d characterizes nonlocality of interaction between the layers. Thus, the exchange interaction between the layers at a given point of the layer plane is determined not by the local thickness of the spacer but rather by its thickness in a region whose dimensions in the spacer layer plane are of the order of d.

We assume that d is much smaller than the other length scales characterizing the magnetic ordering in the structure in question. In other words, we neglect nonlocality and assume that $J_\perp(x, y) \equiv J_\perp(d(x, y))$, where the x and y axes of the Cartesian coordinate system lie in the layer plane and the z axis is normal to it. The edge of a step is taken to be parallel to the y axis.

On one side of the step, we have $J_\perp = J_\perp(n)$, and on the other side, $J_\perp = J_\perp(n-1)$. If $J_\perp(n)J_\perp(n-1) < 0$, frustration occurs in the system. This term is widely used in describing the properties of spin glasses. In the presence of frustration, there is no orientation of spins for which all their pairwise exchange interaction energies are simultaneously minimal. As the simplest example of a frustrated system, we can cite three spins situated at the vertices of a triangle, with all their pairwise interactions being antiferromagnetic (AFM).

In the case considered above, we have a similar situation. A uniform distribution of order parameters (magnetizations in our case) over the layers, which minimizes the exchange energy in each layer, does not minimize the interaction energy between the layers.

The state that arises in this frustrated system will be considered in Section 3.

2.3. Frustration in the Ferromagnet–Antiferromagnet System

In this system, the short-range Heisenberg exchange interaction between spins is dominant. In a ferromagnet–antiferromagnet–ferromagnet three-layered structure, the FM layers interact via the spins of the antiferromagnet; this interaction is much stronger than the RKKY interaction. Therefore, in treating such systems, it will suffice to take into account the nearest neighbor interaction alone. Let us consider the frustration occurring at the interface between an FM and an AFM layer.

The magnetic moment of an antiferromagnet atomic plane parallel to the interface can be either nonzero or zero. In the former case, the antiferromagnet surface is called uncompensated, and in the latter, compensated. For example, for a cubic mirror-symmetric antiferromagnet, the (111) surface is uncompensated, while the (100) and (110) surfaces are compensated. In this review, we consider only the case of an uncompensated antiferromagnet surface, whose roughness causes frustration, as will be shown below. The system consisting of an antiferromagnet with a compensated surface and a ferromagnet is frustrated even if the interface between them is ideally smooth; therefore, the roughness of this interface is of no importance in this respect.

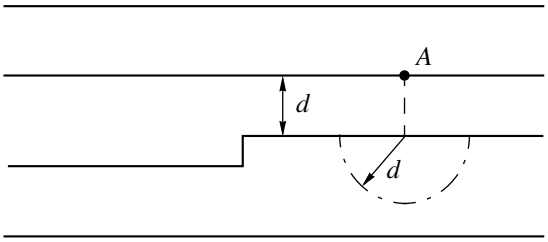

Fig. 5. Atomic step on the interface between layers. The dot-and-dash curve is the boundary of the region making the main contribution to the molecular field at point *A*.

Let us consider the perfectly smooth planar interface between a ferromagnet and an uncompensated antiferromagnet (Fig. 6a). In the ground state and in the absence of an external magnetic field, the spins in the ferromagnet are parallel or antiparallel to the spins located on the top atomic plane of the antiferromagnet depending on the sign of the exchange integral $J_{f,af}$ between neighboring spins belonging to different layers ($J_{f,af} > 0$ corresponds to the parallel orientation).

Now, we consider an atomic step on the interface between a ferromagnet and an uncompensated antiferromagnet (Fig. 6b). The spins of the ferromagnet located on different sides of the step are in contact with antiferromagnet spins belonging to different atomic planes. If the collinear orientation of the FM and AFM order parameters on one side of the step corresponds to a minimum of the interface energy, then this energy on the other side of the step is maximal; therefore, a frustration occurs that is caused by the step.

3. DOMAIN WALLS AND A PHASE DIAGRAM OF A FERROMAGNET–NONMAGNETIC METAL–FERROMAGNET THREE-LAYERED SYSTEM

3.1. A Domain Wall due to Frustration

Let us consider an isolated straight step on one of the interfaces of the three-layered system (Fig. 5). For the sake of definiteness, we assume that

$$J_\perp(x) = \begin{cases} J_1 > 0, & x < 0 \\ J_2 < 0, & x > 0. \end{cases} \quad (3)$$

It is clear that far from the step the mutual orientation of the layer magnetizations must be such that their

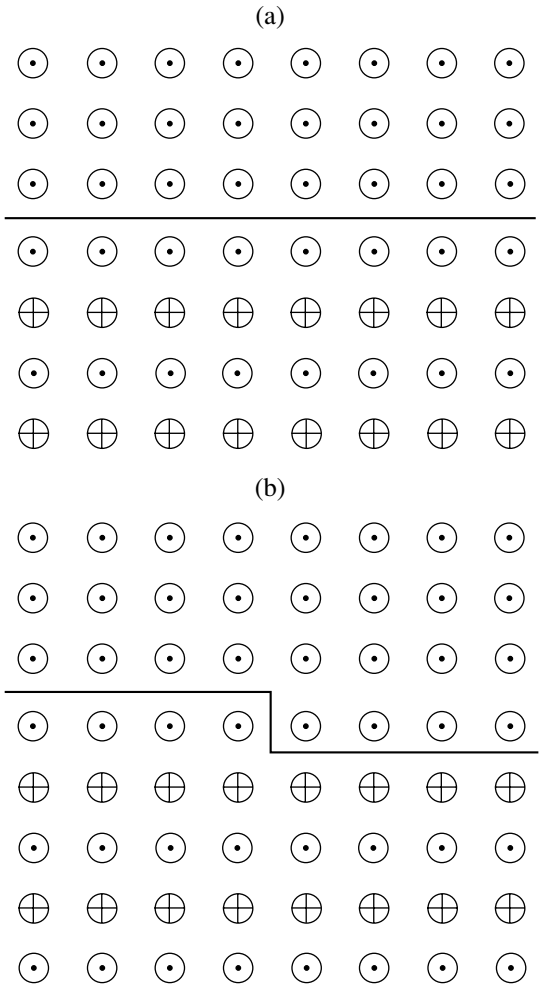

Fig. 6. Interfaces between a ferromagnet and an uncompensated antiferromagnet. (a) Perfectly smooth planar interface and (b) an interface containing an atomic step.

interaction energy is minimal; that is, the magnetizations are parallel to each other for $x \longrightarrow -\infty$ and are antiparallel for $x \longrightarrow +\infty$.

In other words, near the edge of the step a DW arises that runs through all layers and separates the half-space where the layer magnetizations are parallel ($x < 0$) from the half-space of the antiparallel mutual orientation of the magnetizations ($x > 0$).

In this review, we assume that the atomic spins lie in the layer plane; therefore, no stray demagnetizing fields arise in the case of perfectly smooth interfaces. The position of the ith spin is defined by the angle θ_i between the spin and the x axis. The order parameter is assumed not to change in magnitude.

Furthermore, we restrict our consideration to the exchange approximation neglecting anisotropy in the layer plane. This approximation is valid if the exchange energy causing the formation of the DW is much higher than the anisotropy energy and the DW is much thinner than the conventional DW, whose thickness is dictated by the balance between the exchange and anisotropy energies.

The thickness of such a DW of a new type was estimated in [9], and its characteristics were calculated analytically in [10].

The analytical calculation was performed within a continuum approximation. As shown below, the characteristic DW thickness is much larger than the thicknesses of the layers of the nanostructure at hand. Therefore, we can assume that the DW thickness does not vary along the z axis (which is perpendicular to the layer plane). Thus, the problem becomes one-dimensional in the case of a step with a straight edge.

According to [11], the addition to the exchange energy between spins in the layers due to nonuniformity of the order parameter (magnetization) is

$$W_1 = \int\left[\frac{\alpha_1}{2}(\theta_1')^2 + \frac{\alpha_2}{2}(\theta_2')^2\right]d^2\boldsymbol{\rho}, \qquad (4)$$

where θ_i is the tilt angle of the order parameter in the ith FM layer ($i = 1, 2$), the prime denotes differentiation with respect to x, and integration is performed over the surface of the multilayer structure. In order of magnitude, the exchange stiffnesses of the layers α_i are

$$\alpha_i \sim J_i S_i^2 l_i / b, \qquad (5)$$

where J_i is the exchange integral between neighboring spins in the ith layer; S_i is the average value of the atomic spin in this layer; l_i is the thickness of the ith layer; and b is the interatomic distance, which we assume to be the same for all layers.

The interaction energy between the layers in the mean-field approximation is

$$W_2 = -\int\beta(x)\cos(\theta_1 - \theta_2)d^2\boldsymbol{\rho}, \qquad (6)$$

where

$$\beta(x) = \begin{cases}\beta_1 > 0, & x < 0\\ -\beta_2 < 0, & x > 0,\end{cases} \quad \sim J_\perp(x)S_1S_2b^{-2}. \qquad (7)$$

By varying the sum $W_1 + W_2$ with respect to θ_1 and θ_2, we obtain a set of equations

$$\begin{aligned}\alpha_1\theta_1'' - \beta\sin(\theta_1 - \theta_2) &= 0,\\ \alpha_2\theta_2'' + \beta\sin(\theta_1 - \theta_2) &= 0\end{aligned} \qquad (8)$$

with the boundary conditions $\theta_i' \longrightarrow 0$ as $x \longrightarrow \pm\infty$, $\theta_i \longrightarrow 0$ as $x \longrightarrow -\infty$, and $|\theta_1 - \theta_2| \longrightarrow \pi$ as $x \longrightarrow +\infty$. The solution to this set of equations is $\theta_2 = -\alpha_1\theta/(\alpha_1 +$

α_2) and $\theta_1 = \alpha_2\theta/(\alpha_1 + \alpha_2)$, where $\theta(x)$ can be found from the equations

$$\cos\frac{\theta}{2} = -\tanh\left[\left(\frac{\beta_1}{\alpha^*}\right)^{1/2}(x + x_1)\right], \quad x < 0,$$
$$\sin\frac{\theta}{2} = \tanh\left[\left(\frac{\beta_2}{\alpha^*}\right)^{1/2}(x + x_2)\right], \quad x > 0. \tag{9}$$

Here, $\alpha^* = \alpha_1\alpha_2/(\alpha_1 + \alpha_2)$ and the constants x_1 and x_2 can be found from the conditions of continuity of $\theta(x)$ and its derivative $\theta'(x)$ at $x = 0$, which reduces to the equation

$$\tan\frac{\theta}{2}\bigg|_{x=0} = \left(\frac{\beta_2}{\beta_1}\right)^{1/2}. \tag{10}$$

It is easy to see that, for $\beta_1 \gg \beta_2$, the DW is almost entirely located in the region $x > 0$ and, for $\beta_1 \ll \beta_2$, the DW is in the region $x < 0$. In the case of $\alpha_1 = \alpha_2$, the spins of different layers rotate in opposite directions through an angle of 90°. If one of the values of α is much larger than the other (which corresponds to the case where one of the FM layers is much thicker than the other), then the rotation of spins occurs virtually entirely in the thinner layer, whereas in the thicker layer the spins deviate only slightly.

The characteristic DW thickness δ is

$$\delta = \pi\left(\frac{\alpha^*}{\min(\beta_1, \beta_2)}\right)^{1/2}$$
$$\sim \pi b\left(\frac{J_i l_{\min}}{J_\perp b}\right)^{1/2} \sim \pi d\left(\frac{J_i l_{\min}}{J_0 b}\right)^{1/2} \gg d, \tag{11}$$

where $l_{\min}$ is the thickness of the thinner FM layer. For $l/b \sim 3$–5, $J_i/J_0 \sim 1$–10, and $d \sim 10$ Å, we have $\delta \sim 100$ Å, which is much smaller than the DW thickness in iron (800 Å).

If the thickness of this unusual DW is comparable to or larger than the thickness of the conventional DW, then we should include the anisotropy energy $E_a^i = -l_i K_i \cos 2\theta_i$ (for the easy magnetization axis lying in the layer plane) or $E_a^i = -l_i K_i \cos 4\theta_i$ (for the case of a fourfold axis perpendicular to the layer plane). In this case, an order-of-magnitude estimation of the DW thickness gives

$$\delta \sim \pi b^{-1/2}\left(\frac{J_i}{K + J_0/d^2 l_{\min}}\right)^{1/2}. \tag{12}$$

Substituting solution (8) into the functional $W_1 + W_2$, we can find the DW energy integrated over the layer thicknesses, i.e., the energy per unit length of the DW line on the layer surfaces. This energy is equal to the difference between the above-mentioned functional and the sum of the energies of the uniform states with $\theta = 0$ for $x < 0$ and $\theta = \pi$ for $x > 0$ and is found to be

$$\sigma = 4(\alpha^*)^{1/2}[\beta_1^{1/2} + \beta_2^{1/2} - (\beta_1 + \beta_2)^{1/2}]$$
$$\sim d^{-1}S^2[J_i J_0 l_{\min}/b]^{1/2} \sim b^{-1}S^2[J_i J_\perp l_{\min}/b]^{1/2}. \tag{13}$$

Thus, we have calculated the characteristics of an isolated DW in the ferromagnet–nonmagnetic metal–ferromagnet structure.

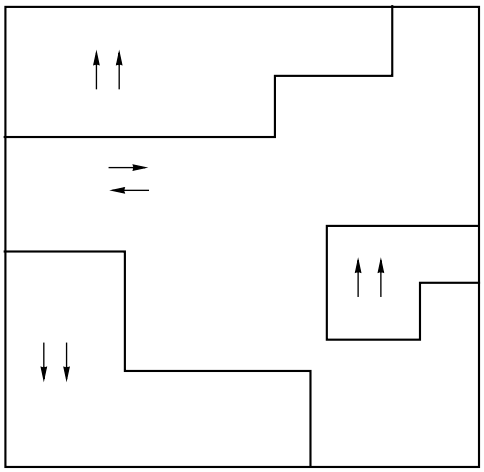

Fig. 7. Domains with parallel and the antiparallel mutual orientation of the magnetizations of FM layers in a three-layered structure.

3.2. Phase Diagram

Now, we investigate the phase diagram for variable interface roughness [12]. If the characteristic distance R between atomic steps on the interface between the layers (giving rise to frustration) is much larger than the DW thickness δ ($R \gg \delta$), then it is energetically favored for the magnetic layers to break up into domains. The domains with parallel and antiparallel mutual orientation of the magnetizations of the FM layers are separated by DWs. The structure pattern of the domain is shown in Fig. 7.

In the opposite extreme case where the characteristic roughness scale is such that $R \ll \delta$, domains cannot form. We restrict our consideration to the case of $R \gg d$, which allows us to use, as before, the local approximation to $J_\perp(\boldsymbol{\rho})$. If $R \ll d$, then $J_\perp(\boldsymbol{\rho})$ is effectively averaged over the region of nonlocality to give $J_\perp(\boldsymbol{\rho}) \approx$ const.

The transition from the state with $R \gg \delta$ to the state with $R \ll \delta$ can occur as the thickness of the spacer layer increases, because $\delta \propto d$. In the case of $R \ll \delta$, the deviations $\psi_i(\boldsymbol{\rho}) = \theta_i(\boldsymbol{\rho}) - \langle\theta_i\rangle$ of the angles θ_i from their average values $\langle\theta_i\rangle$ are small, $|\psi_i| \ll 1$ ($i = 1, 2$).

Now, we show that these deviations are energetically unfavorable in the case of $\langle\theta_1\rangle = \langle\theta_2\rangle$. Indeed, by

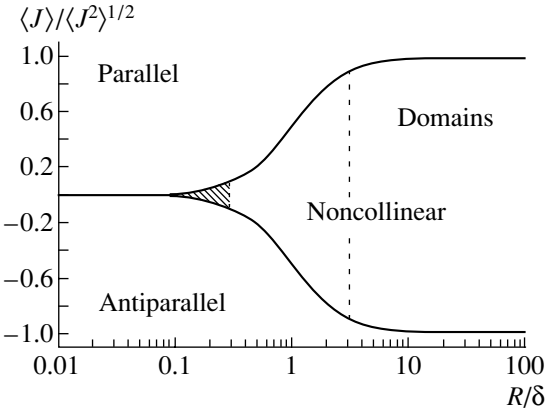

Fig. 8. Exchange–roughness phase diagram for a three-layered system with a nonmagnetic spacer. The region of existence of the noncollinear state is shown by hatching. The dotted line is the boundary of the region of existence of domains.

varying the total energy $W_1 + W_2$ with respect to ψ_i, it is easy to show (following [10]) that ψ_1 and ψ_2 are expressed in terms of the variable $\psi = \psi_1 - \psi_2$ as

$$\psi_1 = \frac{\alpha^*}{\alpha_1}\psi, \quad \psi_2 = -\frac{\alpha^*}{\alpha_2}\psi, \tag{14}$$

$$W_1 = \frac{\alpha^*}{2}\int(\nabla\psi)^2 d^2\boldsymbol{\rho}. \tag{15}$$

When an inhomogeneity occurs with a characteristic maximal magnetization deviation through an angle ψ_0, the specific energy $w_1 = W_1/\sigma$ (σ is the area of the layers) increases by

$$\Delta w_1 \approx \alpha^*\left(\frac{\psi_0}{R}\right)^2, \tag{16}$$

because $|\nabla\psi| \approx \psi_0/R$.

The specific exchange energy between the layers $w_2 = W_2/\sigma$ changes by

$$\begin{aligned}\Delta w_2 &\approx -|J_\perp|S_1S_2b^{-2}(1-\cos\psi_0)\\ &\approx -|J_\perp|S_1S_2b^{-2}\psi_0^2 \approx -\alpha^*\frac{\psi_0^2}{\delta^2}.\end{aligned} \tag{17}$$

If $R \ll \delta$, this gain in energy W_2 is lower than the cost in energy W_1; therefore, in the case of $\langle\theta_1\rangle = \langle\theta_2\rangle$, we have $\psi_1(\boldsymbol{\rho}) = \psi_2(\boldsymbol{\rho}) = 0$.

If $\langle\theta_1\rangle \neq \langle\theta_2\rangle$, then the decrease in W_2 is linear in ψ_0 and is equal to

$$\begin{aligned}\delta w_2 &\approx -J_\perp S_1S_2b^{-2}[\cos(\langle\theta_1\rangle - \langle\theta_2\rangle)\\ &\quad - \cos(\langle\theta_1\rangle - \langle\theta_2\rangle + \psi_0)]\\ &\approx -J_\perp S_1S_2b^{-2}\sin\theta\sin\psi_0 \approx -\alpha^*\frac{\sin\theta}{\delta^2}\psi_0,\end{aligned} \tag{18}$$

where $\theta = \langle\theta_1\rangle - \langle\theta_2\rangle$.

By minimizing the total energy, we find the characteristic value ψ_0 to be

$$\psi_0 \approx \frac{R^2}{\delta^2}\sin\theta, \tag{19}$$

and the decrease in the total energy to be

$$\Delta w_1 + \Delta w_2 \approx -\frac{\langle J_\perp^2\rangle S_1^2S_2^2R^2\sin^2\theta}{\alpha^* b^4} \approx -\frac{\langle J_\perp^2\rangle R^2\sin^2\theta}{J_0 l_{\min} b^3}, \tag{20}$$

where $l_{\min}$ is the smallest of the thicknesses l_1 and l_2 of the FM layers.

Thus, weak nonuniformities of the magnetization distributions over the FM layers become energetically favored in a noncollinear state with $\theta \neq 0$. However, the formation of such a state occurs at a cost in energy of the uniform state because of the term

$$w_2^{(0)} = -\langle J_\perp\rangle S_1S_2b^{-2}\cos\theta. \tag{21}$$

Phenomenologically, this term is interpreted as bilinear exchange. Replacing $\sin^2\theta$ in Eq. (20) by $1 - \cos^2\theta$, we obtain a term proportional to $\cos^2\theta$, which is interpreted as the specific biquadratic-exchange energy

$$w_{BQ} = -J_{BQ}S_1^2S_2^2b^{-2}\cos^2\theta. \tag{22}$$

For the case of periodically arranged steps, the form of the exchange integral J_{BQ} was found in [13]. Note that the exchange integral J_{BQ} is always negative; that is, biquadratic exchange favors the occurrence of a noncollinear state. An order-of-magnitude estimation gives

$$J_{BQ} \approx -\frac{\langle J_\perp^2\rangle R^2}{J_i S^2 l_{\min} b}. \tag{23}$$

A necessary condition for a noncollinear ordered state with $\theta \neq 0$ to arise is

$$|\langle J_\perp\rangle| < 2|J_{BQ}|S_1S_2. \tag{24}$$

Since $|J_1| \approx |J_2| \approx \langle J_\perp^2\rangle^{1/2}$, we can conclude that, to within numerical factors of order unity, inequality (24) is equivalent to the condition

$$\frac{\langle J_\perp\rangle}{\langle J_\perp^2\rangle^{1/2}} < \frac{R^2}{\delta^2}. \tag{25}$$

It is unlikely that the values of J_1 and J_2 and the total area occupied by regions corresponding to spacer thicknesses d_1 and d_2, respectively, satisfy the inequality

$$\frac{\langle J_\perp\rangle}{\langle J_\perp^2\rangle^{1/2}} < 10^{-2}.$$

Therefore, only collinear ordering must occur in multilayer structures with $R \ll \delta$.

The corresponding exchange–roughness phase diagram is shown in Fig. 8. The crosshatched region corresponds to a noncollinear phase in which the layer magnetizations are practically uniform. It is easy to see that the region of parameter values for which this approximation (frequently used in the literature) is adequate is very narrow. As the size R increases (i.e., roughness decreases), the angle ψ_0 of deviation of the magnetization vector from its average direction increases and a continuous transition occurs to a microdomain state.

3.3. The Behavior in a Magnetic Field

Let us consider the behavior of the different phases in a magnetic field applied parallel to the layer plane. The anisotropy in the layer plane is assumed to be negligible.

For the phase in which the magnetizations of the FM layers are parallel to each other, narrow square hysteresis loops will be observed (Fig. 9a).

In the phase with antiparallel mutual orientation of the magnetizations of the two identical FM layers, the total magnetization will increase smoothly with the magnetic field (Fig. 9b). This behavior is identical to that of a mirror-symmetric two-sublattice antiferromagnet with intersublattice exchange energy β. The angle between the magnetization vectors of the FM layers can be found by minimizing the energy:

$$\tilde{W} = -2M_0 lB\cos\theta - \beta\cos 2\theta, \qquad (26)$$

where M_0 is the magnetization of the FM layers, l is their thickness, $\beta < 0$, and θ is the angle between the magnetic induction and the magnetic moment of an FM layer (Fig. 3b).

It is easy to see that saturation occurs in a magnetic field

$$B_{\text{sat}} = \frac{2|\beta|}{M_0 l}. \qquad (27)$$

In the region where a microdomain state exists, the magnetization curve, in a first approximation, will be a superposition of the curves described above with the weights corresponding to the volume fractions of the domains with parallel and antiparallel mutual orientations of the layer magnetizations (Fig. 9c).

If the structure under study exhibits a magnetization curve of this type, there is a good probability that this structure is in a microdomain state. The small crosshatched region in Fig. 8 corresponds to another possible state.

3.4. Experimental Observations

Hysteresis loops similar to that shown in Fig. 9c have been observed in many studies (see, e.g., [14, 15]). However, such curves were interpreted in terms of biquadratic exchange and the magnetic microstructure, as a rule, was not examined. Microdomains with parallel and antiparallel mutual magnetization orientations were observed using spin-polarized low-energy electron microscopy (SPLEEM) [16]. It was found that the boundaries between microdomains coincide with the boundaries of atomic terraces on interfaces. Microdomains can also be observed using transmission electron microscopy [17], spin-polarizing scanning tunneling microscopy [18], and magnetic-force microscopy.

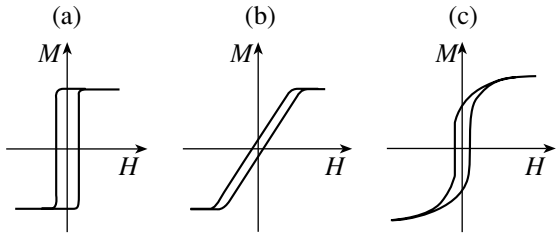

Fig. 9. Hysteresis loops in the regions of the phase diagram corresponding (a) to the parallel and (b) antiparallel mutual orientation of the magnetizations of the FM layers and (c) to the microdomain state.

It is of considerable interest to make *in situ* measurements of the relief of the layer surface before sputtering the next layer and then to investigate the magnetic microstructure, magnetization curves, and magnetoresistance.

4. FERROMAGNET–ANTIFERROMAGNET TWO-LAYER SYSTEM

In contrast to the case considered above, the spins of the AFM layer in this system are ordered and are characterized by their own exchange stiffness. The type of DWs caused by frustration essentially depends on the relationship between the exchange stiffnesses of the ferromagnet and antiferromagnet (see below).

4.1. Model

We assume that the AFM order parameter **L**, which is the difference between the magnetizations of the sublattices, lies in the layer plane and, as before, is specified by the angle that the vector **L** makes with the x axis ($|\mathbf{L}| = \text{const}$).

In this case, the contribution to the exchange energy of each layer coming from nonuniformities in the distribution of the order parameter over the layer can be represented in the form [11]

$$W_i = \frac{J_i S_i^2}{2b}\int(\nabla\theta_i)^2 dV, \qquad (28)$$

where integration is performed over the volume of the layer.

Here, in contrast to the preceding section, the problem is not one-dimensional. Indeed, the DW thick-

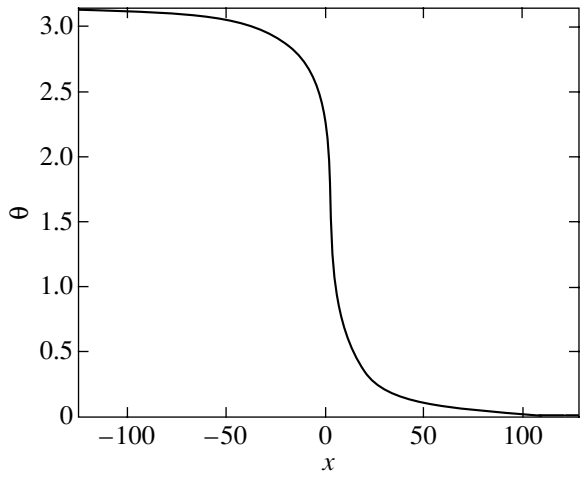

Fig. 10. Typical variation in the tilt angle of the order parameter through the DW thickness.

nesses, as shown below, are comparable to atomic-scale lengths in this case and significantly vary with the distance from the interface. Therefore, even in the case of an atomic step with an infinite edge, the problem is two-dimensional.

By varying expression (28) with respect to the parameter θ_i, we obtain an equation for the order parameter in the interior of the *i*th layer [19],

$$\Delta\theta_i = 0. \tag{29}$$

In order to find the boundary conditions, one should write the interaction energy between spins situated near the interface in the discrete representation and differentiate this energy with respect to the rotation angle of the particular spin. After passing to the continuum representation, we thus obtain

$$\tilde{\Delta}\theta_i - \frac{\partial\theta_i}{\partial n} = \pm\frac{J_{f,af}S_{i+1}}{J_iS_i}\sin(\theta_i - \theta_{i+1}), \tag{30}$$

where $\tilde{\Delta}$ is the two-dimensional Laplacian in the layer plane, $\frac{\partial}{\partial n}$ is the derivative along the outward normal to the layer, and $J_{f,af}$ is the exchange constant characterizing the interaction between spins belonging to different layers; all distances are measured in units of the interatomic distance *b*. The plus and minus signs on the right-hand side of Eq. (30) correspond to spins lying on different sides of the atomic step at the interface, respectively. For the free surface, the right-hand side of Eq. (30) vanishes.

If we vary the interaction energy between the layers with respect to θ_i in the continuum representation, we will arrive at an equation that does not contain the first term on the left-hand side of Eq. (30) and, therefore, does not reduce to Eq. (29) in the case where the adjacent layers are identical.

The exchange interaction energy between the adjacent layers is

$$W_{i,i+1} = \pm\frac{J_{f,af}S_iS_{i+1}}{b^2}\int\cos(\theta_i - \theta_{i+1})d^2\boldsymbol{\rho}, \tag{31}$$

where integration is performed over the interface between the layers. The plus and minus signs on the right-hand side of Eq. (31) correspond to those in Eq. (30).

4.2. Domain Wall in a Ferromagnetic Film on an Antiferromagnetic Substrate

Let us consider a thin FM film deposited on a much thicker AFM substrate (or a thin AFM film deposited on a thick FM substrate). In the exchange approximation, the latter problem will reduce to the former, in which we replace the indices $f \rightleftharpoons af$. A DW that arises in this case is described by the following three dimensionless parameters: the film thickness $a = l_f/b$; the quantity

$$\alpha_f = \frac{J_{f,af}S_{af}}{J_fS_f}, \tag{32}$$

which characterizes the ratio of the exchange interaction energy between neighboring spins belonging to different layers to the exchange interaction energy between adjacent spins belonging to the FM layer; and the quantity

$$\gamma = \frac{J_fS_f^2}{J_{af}S_{af}^2}, \tag{33}$$

which is the ratio between the exchange energies in the film and in the substrate.

Equations (29) and (30) form a set of Laplace equations with nonlinear boundary conditions. These equations were solved numerically in [20, 21] using a method similar to integral transformation.

The orientation of the coordinate system is similar to that chosen in Subsection 2.2; namely, the *y* axis coincides with the edge of a step and the *z* axis is perpendicular to the film plane. The plane $z = 0$ coincides with the film–substrate interface, and the plane $z = a$ is the free surface of the film. In the region $x \ll -\delta_f$ (δ_f is the DW thickness), we have $\theta_{af} = \theta_f = 0$, and in the region $x \gg \delta_f$, we have $\theta_{af} = 0$ and $\theta_f = \pi$. From the symmetry of the problem, it follows that $\theta_{af} = 0$ and $\theta_f = \pi/2$ at $x = 0$.

First, let us consider the case where $\gamma \ll 1$ and, therefore, the exchange stiffness of the substrate is much higher than that of the film [20]. In this case, the distribution of the order parameter over the substrate is virtually uniform. The typical $\theta(x)$ dependence in the region $0 < z < a$ is shown in Fig. 10. Note that at $x = z = 0$ the derivative θ''_{xx} is discontinuous, while θ'_z remains continuous. The DW thickness $\delta_f(z)$ is defined as the

distance between the points with coordinates (x_1, z) and (x_2, z) corresponding to the values $\theta_1 = \pi/4$ and $\theta_2 = 3\pi/4$, respectively.

The main feature of the DWs under study is that their thickness increases with distance from the interface. The $\delta_f(z)$ dependence for $\alpha_f a \gg 1$ is shown in Fig. 11. It can be seen that this dependence is linear near the substrate, whereas near the free surface the DW thickness δ_f virtually does not vary. In the opposite case of $\alpha_f a \ll 1$, the variation of the DW in thickness is insignificant.

The dimensionless DW thickness $\delta_0^f = \delta_f(z = 0)$ and the thickness-averaged value of $(\delta_f)_z'$, which we denote as $\tilde{\beta}$ in what follows, can be estimated using simple energy arguments. Indeed, let us approximate $\theta(x, z)$ by the function

$$\theta(x, z) = \begin{cases} \pi, & x \geq \delta_f(z), \\ \frac{\pi}{2}(1 + x/\delta_f(z)), & -\delta_f(z) < x < \delta_f(z) \\ 0, & x \leq -\delta_f(z), \end{cases} \quad (34)$$

where

$$\delta_f(z) = \delta_0^f + \tilde{\beta} z, \quad 0 \leq z \leq a. \quad (35)$$

The contribution to the energy (per unit length of the DW along the y axis) from nonuniformities of the order parameter in the DW is

$$w_1 = \frac{J_f S_f^2}{2b} \int_0^a dz \int_{-\infty}^{\infty} dx [(\theta_x')^2 + (\theta_z')^2] \approx \frac{\pi^2 J_f S_f^2}{4b} \left(\frac{1}{\tilde{\beta}} + \frac{\tilde{\beta}}{3} \right) \ln \frac{\tilde{\beta} a + \delta_0^f}{\delta_0^f}. \quad (36)$$

Due to the step, the interaction energy between the film and substrate increases by the quantity

$$w_2 = \frac{2 J_{f,af} S_f S_{af}}{b} \int_0^{\infty} dx [1 - \cos\theta(x, 0)] \approx \frac{2 J_{f,af} S_f S_{af}}{b} \delta_0^f. \quad (37)$$

Minimizing the energy w_1 with respect to the parameter $\tilde{\beta}$ and then minimizing the total DW energy $\tilde{w} = w_1 + w_2$ with respect to the parameter δ_0^f, we can find these parameters. The result is

$$\tilde{\beta} \sim \sqrt{\alpha_f a}, \quad (38)$$

$$\delta_0^f \sim \sqrt{a/\alpha_f} \quad (39)$$

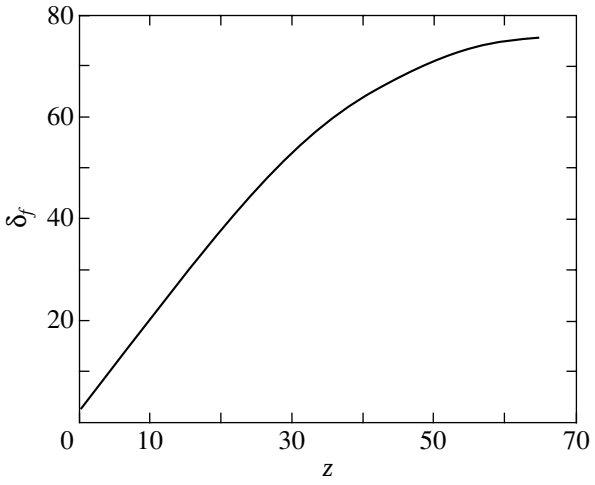

Fig. 11. Typical variation in the DW thickness with distance from the interface for $\alpha_f a \gg 1$ ($\alpha_f = 1$, $a = 64$).

in the case of $\alpha_f a \ll 1$ and

$$\tilde{\beta} \sim 1, \quad (40)$$

$$\delta_0^f \sim 1/\min(1, \alpha_f) \quad (41)$$

for $\alpha_f a \gg 1$. The continuum approximation is valid if $\delta_0^f \gg 1$.

The characteristic DW thickness $\delta_f(a/2)$ is found to be

$$\delta_f\left(\frac{a}{2}\right) \sim \begin{cases} \delta_0^f \sim \sqrt{a/\alpha_f}, & \alpha_f a \ll 1 \\ a, & a\alpha_f \gg 1. \end{cases} \quad (42)$$

It is significant that for $a \sim 10$–100 Å the DW thickness δ_f is much smaller than the thickness of a conventional DW, because the value of δ_f is determined by the balance between the exchange energies rather than between the exchange and anisotropy energies.

The DW energy per unit length is estimated to be

$$\tilde{w} \sim \begin{cases} \frac{J_f S_f^2}{b} \sqrt{\alpha_f a}, & \alpha_f a \ll 1 \\ \frac{J_f S_f^2}{b} \ln(\alpha_f a), & \alpha_f a \gg 1. \end{cases} \quad (43)$$

Due to the DW broadening, the DW energy increases with the thickness of the film only logarithmically for $\alpha_f a \gg 1$.

Now, we consider the case where $\gamma \gg 1$ and, therefore, the exchange stiffness of the film is much higher than that of the substrate. If $\gamma^2 a \alpha_f \ll 1$, then the order parameter of the substrate is affected only slightly and the DW parameters are similar to those found in the case of $\alpha_f a \ll 1$.

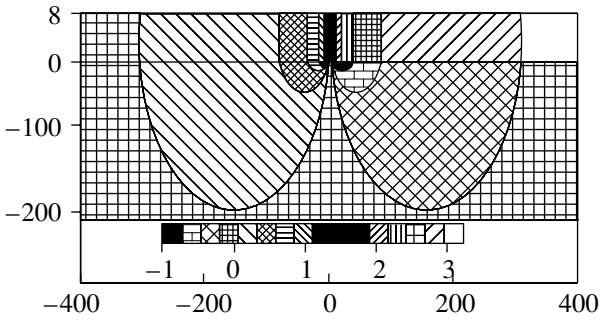

Fig. 12. Distribution of the order parameters over a DW. The ordinate is equal to zero at the film–substrate interface. All distances are reduced to the lattice parameter. The correspondence between the hatching and the value of θ_i (measured in radians) is shown in the inset.

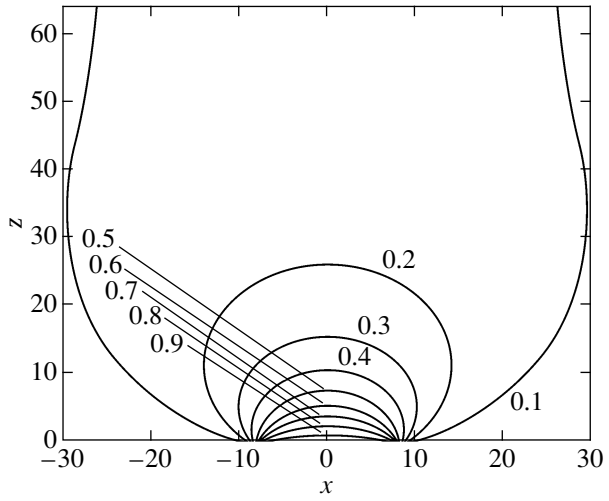

Fig. 13. Static spin vortex in the film near the film–substrate interface in the case of $a \gg R$. The lines of constant values of θ_f are labeled by the values of θ_f measured in units of π.

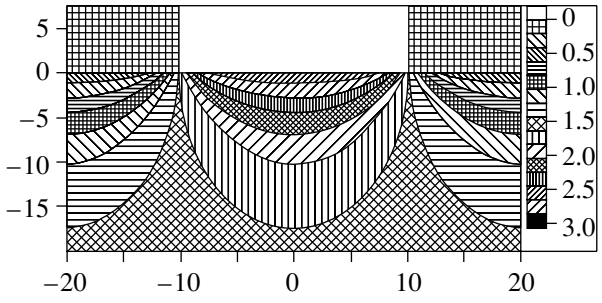

Fig. 14. Distribution of the order parameters in the vortex phase. The ordinate is equal to zero at the film–substrate interface. All distances are reduced to the lattice parameter. The correspondence between the hatching and the value of θ_i (measured in radians) is shown in the inset.

In the opposite case of $\gamma^2 a\alpha_f \gg 1$, the order parameter of the substrate is distorted and two characteristic lengths arise. One of them is the DW thickness in the FM layer

$$\delta_f \approx \gamma a. \tag{44}$$

Since $\delta_f \gg a$, the DW broadening in the ferromagnet can be neglected. The other characteristic length is the thickness δ_0^{af} of the region near the film–substrate interface in which the quantity $\theta_f - \theta_{af}$ differs from its optimum value (0 for $x < 0$ and π for $x > 0$):

$$\delta_0^{af} \approx (1 + \gamma\alpha_f)/\gamma\alpha_f, \quad \delta_f \gg \delta_0^{af}. \tag{45}$$

In the region $|x| < \delta_f$ and $|z| < \delta_f$, vortical distortions of the AFM order parameter arise in the substrate (Fig. 12). The DW energy per unit length in this case is

$$w \approx \frac{J_{af} S_{af}^2}{b} \ln \frac{\delta_f}{\delta_0^{af}}, \tag{46}$$

with the dominant contribution to it coming from the order parameter distortions in the substrate.

If the substrate thickness $d_{af} < \gamma a$, then the DW runs through it; therefore, the AFM layer breaks up into domains, while the FM layer remains virtually uniform. In other words, the pattern is the same as that in the case of $\gamma \ll 1$ but the layers exchange places.

Thus, we have found the critical thickness above which the substrate can be considered thick. If the distance between the steps is large, we have $d_{af}^* = \gamma a$.

4.3. Phase Diagram

Atomic steps break up the film–substrate interface into regions of two types. In the first type of region, the interface energy is minimal when the FM and AFM order parameters are parallel to each other, and in the second type, the interface energy is minimal when these order parameters are antiparallel.

If the characteristic spacing between the steps is much larger than its critical value, $R \gg \delta_f(a/2)$, then the film breaks up into microdomains, with their boundaries coinciding with the edges of the atomic steps [22, 23]. The magnetizations in adjacent domains are oppositely directed, and their direction corresponds to a minimum value of the interface energy.

In the case of $R \ll \delta_f(a/2)$, DWs overlap; therefore, domains cannot form and the film passes into a single-domain state. For $\gamma \ll 1$ and $a\alpha_f \ll 1$ or for $\gamma \gg 1$ and $\gamma^2 a\alpha_f \ll 1$, order-parameter distortions are small in both the film and the substrate.

If $\gamma \ll 1$, $a\alpha_f \gg 1$, and $\delta_0^f \ll R \ll a$, then specific static spin vortices arise near the substrate (Fig. 13). These vortices penetrate a distance of the order of R into the film, while in the other part of the film the uni-

form distribution of the order parameter remains unperturbed. In the case of $\gamma \gg 1$, $\gamma^2 a\alpha_f \gg 1$, and $\delta_0^{af} \ll R \ll \delta_f$, the film remains uniform and analogous spin vortices arise in the substrate near the interface (Fig. 14). Each vortex is confined by the edges of steps and becomes progressively wider as the distance from the steps increases. The vortex size in the direction perpendicular to the interface is of the order of R.

For smaller values of R, the state of the system corresponds to the region of weak distortions in the phase diagram.

Let us consider the mutual orientation of the FM and AFM order parameters in the vortex phase. As mentioned above, steps break up the entire interface into regions of two types. We denote their total areas by σ_1 and σ_2, respectively. Let ψ be the angle between the average magnetization of the FM film and the AFM order parameter in the substrate bulk. The difference $\theta_f - \theta_{af}$ varies from zero to ψ in a vortex occupying a region of the first type and from ψ to π in a vortex occupying a region of the second type.

By analogy with the "magnetic proximity" model proposed by Slonczewski [24], we represent the energy of the system in the form

$$W = C_1\psi^2 + C_2(\pi - \psi)^2, \tag{47}$$

where, according to [19, 25, 26],

$$C_j \equiv C\sigma_j \approx \frac{\min(J_f S_f^2, J_{af} S_{af}^2)\sigma_j}{Rb}. \tag{48}$$

In the case of $\sigma_1 = \sigma_2$, the equilibrium film magnetization must be perpendicular to the AFM order parameter in both the vortex phase and the weak-distortion region if the external magnetic field is zero and the anisotropy energy due to steps is ignored.

The thickness–roughness phase diagram for the film–substrate system is shown in Fig. 15. It should be noted that the transition from the multidomain to the single-domain state that occurs in the film as the parameter R decreases is continuous and, strictly speaking, is not a phase transition. If $\gamma \gg 1$ and, therefore, the Curie temperature of the ferromagnet is higher than the Néel temperature of the antiferromagnet, this transition can be initiated by heating the sample. As the Néel temperature is approached, the DW thickness $\delta_f \propto \gamma \propto T_N/(T_N - T)$ increases indefinitely and the transition to the single-domain state occurs.

4.4. The Behavior in a Magnetic Field

Now, we consider the behavior of the phases in an external magnetic field.

When the FM film is in the single-domain state, the application of an external magnetic field directed at an angle to the spontaneous magnetization causes the magnetization vector to rotate everywhere in the film plane. We restrict ourselves to the case where the film thickness is fairly small and, therefore, the magnetization rotation is accompanied by the formation of a conventional DW, which is parallel to the film–substrate interface and positioned in the AFM substrate near the interface. In the case of a thick film, a conventional DW can initially arise, for certain relationships between the model parameters, in the film itself near the interface with the substrate. The situation is fully analyzed in our papers [25, 26].

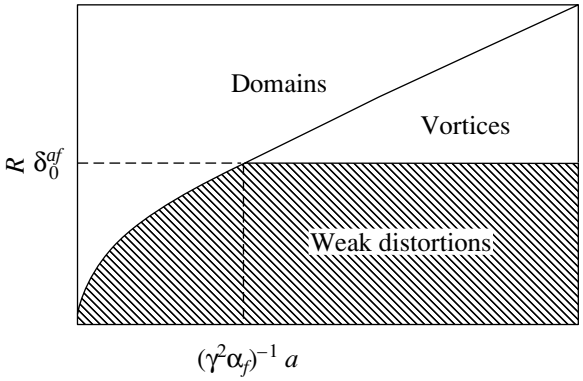

Fig. 15. Thickness–roughness phase diagram for the film–substrate system.

Since the gain in the Zeeman energy of the film in an external magnetic field must compensate for the cost of producing a DW, the magnetization rotation will begin in a magnetic field that is equal, in order of magnitude, to [27, 28]

$$B_{af}^0 \sim \frac{\sigma_{af}}{Ma}, \tag{49}$$

where σ_{af} is the surface energy density of a conventional DW in the antiferromagnet and M is the magnetization of the film. Therefore, the magnetization curve is biased to the range of negative fields (with respect to the magnetization direction in the absence of a magnetic field) by the quantity B_{af}^0. This effect of an AFM substrate is called unidirectional anisotropy. A great number of papers have been dedicated to this phenomenon (see, e.g., review [29]). However, it is beyond the scope of the present review to discuss this effect. The width of the field range within which the magnetization reversal occurs is also of the order of B_{af}^0.

The unidirectional anisotropy does not arise in the multidomain phase. In an external magnetic field aligned with or opposed to the magnetization of domains (we call them domains of the first and second types, respectively), the magnetization in domains of the first type remains unchanged, while the magnetization of the second-type domains rotates through an angle of 180°. If the domain size R is larger than the thickness Δ_{af} of a conventional DW in the antiferromag-

net, then this rotation is accompanied by the formation of such a DW in the substrate near the interface with the film; the characteristic field of the magnetization reversal is of the order of B_{af}^0.

In the case of $R \ll \Delta_{af}$, the magnetization rotation in a domain is accompanied by the formation of a static spin vortex in the AFM substrate; the characteristic magnetization reversal field is of the order of $B_{af}^0 \Delta_{af}/R$. In addition to the vortex, a 90° DW arises in the substrate. The reason for its formation is analogous to that for the film magnetization in the single-domain state being perpendicular to the order parameter in the substrate bulk in the absence of an external magnetic field; namely, the formation of a DW reduces the energy of the vortex system.

Indeed, in the absence of a DW, no vortices arise in domains in which the magnetization is parallel to the external magnetic field, whereas in domains with the initial antiparallel orientation of the magnetization with respect to the magnetic field a 180° vortex forms when the field becomes equal to $B_{af}^0 \Delta_{af}/R$. In the presence of a 90° DW, vortices arise in both types of domain, with the AFM order parameter twisting in opposite directions in domains of different types. Since the energy of a vortex is proportional to the twist angle, the formation of a DW decreases the vortex energy, and this decrease in energy due to the DW is larger than the energy required for the DW formation [26].

If a magnetic field is applied in the film plane at right angles to the magnetization of domains, the characteristic magnetization reversal field is of the same order of magnitude as in the case of a magnetic field applied along the domain magnetizations; however, in the former case, a 90° DW does not form, because static 90° vortices with the AFM order parameter twisting in opposite directions arise in both types of domains.

4.5. Experimental Data

The magnetization pattern discussed in Subsection 4.3 agrees with the data from [30], where the thickness–vicinal angle β' phase diagram was investigated for an iron film deposited on Cr(001). For β' close to zero, the multidomain phase was observed at film thicknesses $a < a_c = 3.5$ nm. In a film with critical thickness a_c, the characteristic distance R between the edges of randomly arranged steps is equal to γa. For large values of a, a single-domain phase was observed in which the magnetization was perpendicular to the edges of steps. According to the theory described above, the antiferromagnetism vector must be parallel to steps. It is of interest to determine its orientation experimentally.

If $\beta' \neq 0$, there are not only randomly arranged atomic steps but also regularly arranged parallel steps. When the concentration of the latter steps becomes dominant (at $\beta' \geq 1°$), the value of a_c begins to decrease. According to the theory described above, $a_c \approx R/\gamma \propto \tan^{-1}\beta' \propto (\beta')^{-1}$.

At large values of β', an orientational phase transition to a phase in which the magnetization was parallel to steps was observed [30]. This transition was due to the anisotropy induced by steps through relativistic effects, e.g., through dipole–dipole interaction [31].

5. FERROMAGNET–ANTIFERROMAGNET–FERROMAGNET THREE-LAYERED SYSTEM

In this section, we restrict ourselves to the case of $\gamma \gg 1$, where the exchange stiffness of the AFM spacer layer is lower than that of the FM layers. In the opposite extreme case (for approximately equal layer thicknesses), the problem for each interface between the layers reduces to that for a two-layer system. To reduce the number of model parameters, we assume the thicknesses of all layers to be equal.

5.1. Domain Walls

DWs run through each of the three layers, and their coordinates in the layer plane coincide with those of the edges of atomic steps at any of the two interfaces. The magnetization vector in a DW rotates in opposite directions in different FM layers. The AFM order parameter rotates together with the magnetization of that FM layer at whose interface with the AFM spacer there is no step at the given site.

The structure and energy of a DW depend on the parameter $\gamma\alpha_f a$ [21]. In the case of $\gamma\alpha_f a \ll 1$, the $\theta_{f(af)}(z)$ dependence (i.e., the DW broadening) can be neglected and the problem becomes one-dimensional.

The quantity $|\nabla\theta_f|$ in a DW is of the order of δ_f^{-1}. Using Eq. (28), the energy per unit DW length w_1 can be found to be

$$w_1 = \frac{J_f S_f^2 a}{b\delta_f}. \tag{50}$$

The angle between spins belonging to different layers differs significantly from its value corresponding to the minimum interaction energy between the layers in the region $|x| < \delta_f$. The increase in the interaction energy between the layers (per unit DW length) is equal to

$$w_2 = \frac{J_{f,af} S_f S_{af} \delta_f}{b}. \tag{51}$$

Minimizing the sum $w_1 + w_2$, we find

$$\delta_f \approx \sqrt{a/\alpha_f}. \tag{52}$$

In the AFM spacer layer, the DW thickness is $\delta_{af} \approx \sqrt{a/\gamma\alpha_f} = \delta_f/\sqrt{\gamma} \ll \delta_f$. The distribution of the order

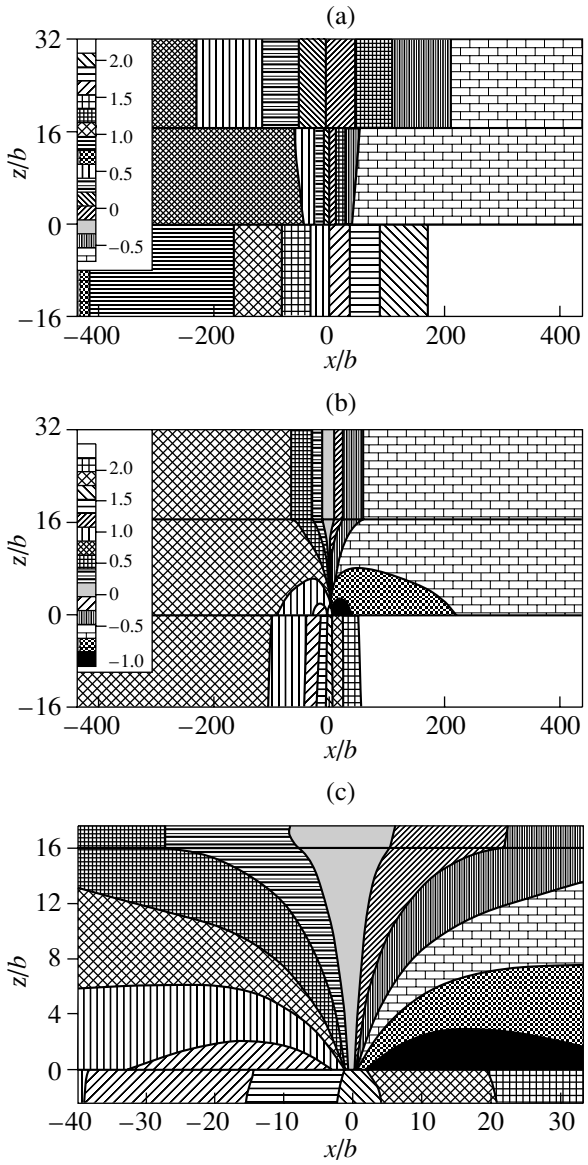

Fig. 16. Domain wall in the ferromagnet–antiferromagnet–ferromagnet three-layered system in the case of (a) $\gamma\alpha_f a \ll 1$ and (b) $\gamma\alpha_f a \gg 1$. The correspondence between the hatching and the value of θ_i (measured in radians) is shown in the inset. Panel (c) shows the central fragment of panel (b). Coordinates $z = 0$ and 16 correspond to the interfaces between the layers. The step is located at the point $x = 0$ and $z = 0$.

parameters over the DW is shown in Fig. 16a. The DW energy per unit length is

$$w \approx \frac{J_f S_f^2}{b}\sqrt{a\alpha_f} \sim \frac{S_f}{b}\sqrt{aJ_f J_{f,af} S_f S_{af}}. \qquad (53)$$

Exact numerical calculations of δ_f and w performed in a wide range of values of α_f and a lend support to the validity of the estimates presented above (and of the results discussed below).

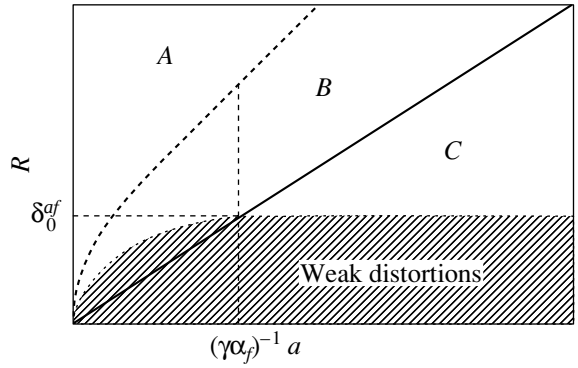

Fig. 17. Phase diagram of the ferromagnet–antiferromagnet–ferromagnet three-layered system. The solid and dashed lines correspond to $R = a$ and $R = \delta_f'$, respectively. The hatched region corresponds to weak order parameter distortions.

In the opposite extreme case of $\gamma\alpha_f a \gg 1$, the DW thickness in the AFM spacer increases significantly with distance from the interface containing an atomic step. The distribution of the order parameters over the DW in this case is shown in Fig. 16b. The characteristic parameters of this distribution can be estimated in the same way as in the case of $\gamma\alpha_f a \ll 1$. The dominant contribution to the DW energy comes from order parameter distortions in the antiferromagnet. In the region $|x| \le a$, the quantity $|\nabla\theta_{af}|$ varies inversely with the distance from the step, whereas in the region $a \ll |x| \ll \delta_f'$ (δ_f' is the DW thickness in the FM layers) the lines of constant values of θ_{af} are almost parallel to the interfaces (Fig. 16c). In this region, we have $|\nabla\theta_{af}| \approx a^{-1}$.

The minimum value of the DW thickness in the antiferromagnet is $\delta_0^{af} = (1 + \gamma\alpha_f)/\gamma\alpha_f$, the derivative is $\partial\delta_{af}/\partial z \approx 1$ near the step, and the quantity δ_f' is given by

$$\delta_f' \approx a\sqrt{\gamma} \gg a. \qquad (54)$$

The DW energy per unit length is

$$w \approx \frac{J_{af} S_{af}^2}{b}\left(\sqrt{\gamma} + \frac{\pi}{2}\ln\frac{a}{\delta_0^{af}}\right). \qquad (55)$$

It is easy to see that δ_0^{af} is of the order of the interatomic distance and that the average DW thickness is of the order of tens of angstroms; therefore, the DWs due to frustration are much thinner than conventional DWs in a ferromagnet, where the DW thickness is dictated by the balance between the exchange and anisotropy energies.

5.2. Phase Diagram

The three-layered system can be in the following three different phases (Fig. 17).

5.2.1. Phase A. At large values of the parameter $R > \delta_f$ (δ_f'), all layers break up into domains with parallel and antiparallel mutual orientations of the magnetizations of the FM layers. Note that, in the case of an AFM spacer, the domains can be much smaller in size than in the case of a nonmagnetic spacer, where the domain size is of the order of tenths of a micrometer.

For $a \sim 10$ Å and $\gamma \sim 3$, the condition $R > \delta_f(\delta_f')$ is satisfied even for domain sizes as small as several hundreds of angstroms. Therefore, the system is in a nanodomain rather than microdomain state in this case; significantly subtler techniques are required to examine such states. This fact can be the reason why such domain structures have not been observed in three-layered systems with an AFM spacer layer.

5.2.2. Phase B. As the parameter R decreases, DWs begin to overlap and, at the critical value $R_c = \delta_f(\delta_f')$, a continuous transition occurs to a state in which the FM layers are almost uniformly magnetized. In this state (we refer to it as phase *B*), the additional energy relative to the energy of the state without frustration is associated either with order parameter distortions in the AFM spacer or with the interaction energy between the layers. Near the Néel temperature of the spacer T_N (which is lower than the Curie temperature of the ferromagnet), we have $\gamma \propto T_N/(T_N - T)$; therefore, the $A \longrightarrow B$ transition can be initiated by heating the system from a temperature $T_0 < T_N$.

Note that the Slonczewski magnetic-proximity model is applicable in the range of values of R where phase *B* exists [24].

In the range $\max(a, \delta_0^{af}) \ll R \ll R_c$, the dependence of the energy of the system on the angle ψ between the magnetization vectors of the FM layers is described by Eq. (47) in the case of $\gamma\alpha_f a \gg 1$. The constants C_1 and C_2 can be estimated to be [32]

$$C_{1,2} = \frac{J_{af}S_{af}^2}{2a}\frac{\sigma_{1,2}}{b^2}, \qquad (56)$$

where σ_1 and σ_2 are the total areas of the regions of the first and second types, respectively, on the surface of the spacer layer.

In the opposite extreme case of $\gamma\alpha_f a \ll 1$, the interaction energy between the layers is

$$W = -\frac{2J_{f,af}S_fS_{af}}{b^2}\left(\sigma_1\cos\frac{\psi}{2} + \sigma_2\cos\frac{\pi-\psi}{2}\right). \qquad (57)$$

If $\sigma_1 = \sigma_2$, the energy reaches its minimum at $\psi = \pi/2$; therefore, in the absence of an external magnetic field, the magnetizations of the FM layers are perpendicular to each other.

In contrast to phase *A*, where the energy of the system is independent of the direction of order parameter rotation in a DW, the situation is quite different in phase *B*. Indeed, as DWs begin to overlap, the degeneracy with respect to the direction of rotation is lifted and a large number of metastable states arise that differ in the direction and angle of rotation of the AFM order parameter in certain regions confined by atomic steps.

As the parameter R is decreased further in the case of $\gamma\alpha_f a \ll 1$, the system transforms into a state with weak distortions in the range $a \ll R \ll \delta_{af}$. In this state, the order parameters are almost uniform, the magnetizations of the FM layers remain perpendicular to each other, and the energy W decreases by a factor of $(R/\delta_{af})^2$ with respect to its value given by Eq. (57).

5.2.3. Phase C. Now, we consider the range $R \ll a$. In this case, all distortions are concentrated near the interfaces, the interaction between the FM layers becomes weak, and the interaction energy between adjacent layers is of primary importance. This energy is considered in [15] for a two-layer system.

If $\sigma_1 = \sigma_2$, the AFM order parameter is directed at right angles to the (collinear) magnetizations of the FM layers (phase *C*).

In the case of $\gamma\alpha_f a \gg 1$, static vortices form in the AFM spacer layer near the interfaces if $\delta_0^{af} \ll R \ll a$ (Fig. 14). For smaller values of R, the system transforms into a state with weak distortions.

In the case of $\gamma\alpha_f a \ll 1$, the transition from phase *B* to phase *C* occurs when the system is in a state with weak distortions. Both phases *B* and *C* are characterized by a large number of metastable states. The computer simulation performed in [21] showed that the transition from phase *B* to phase *C* is a first-order phase transformation. These phases coexist in a certain range of values of R, and their energies become equal at a certain value $R^* \sim a$. This value is independent of temperature; therefore, the $B \longrightarrow C$ phase transition cannot be initiated by varying the temperature of the system.

5.3. The Behavior in a Magnetic Field

The magnetization reversal occurs almost independently in the FM layers in phase *C*. Therefore, the hysteresis loop must coincide with that for a two-layer system consisting of an FM and an AFM layer. Here and henceforth, we assume that the maximum magnetic field is much lower than the exchange field in an antiferromagnet. Therefore, the magnetization of AFM layers can be ignored.

If the applied magnetic field is weak but higher than the anisotropy field in the plane of the FM layers, then the magnetization vectors of the FM layers in phase *B* make an angle of 45° with the external field and remain

virtually perpendicular to each other. The magnetization of the system is equal to $M_{\max}/\sqrt{2}$, where $M_{\max}$ is the maximum magnetization of the FM layers. The further evolution of the system can be studied by minimizing the sum of the interaction energies of the FM layers with each other [Eq. (47) or (57)] and with the external magnetic field. The energy of the FM layers in an external magnetic field B is

$$W_f = -2MaBb(\sigma_1 + \sigma_2)\cos\frac{\psi}{2}. \quad (58)$$

In the case of $\sigma_1 = \sigma_2$, $R \gg \delta_0^{af}$, and $\gamma a \alpha_f \gg 1$, the angle ψ between the magnetizations of the FM layers can be found from the transcendent equation

$$\frac{J_{af}S_{af}^2}{ab^2}\left(\frac{\pi}{2} - \psi\right) = MaBb\sin\frac{\psi}{2}. \quad (59)$$

The characteristic field B^*, in which the magnetization changes significantly, is

$$B^* \sim \frac{J_{af}S_{af}^2}{Ma^2b^3}. \quad (60)$$

This field is much lower than the exchange field of the antiferromagnet if the temperature is not in the immediate vicinity of T_N.

If $\gamma a \alpha_f \ll 1$, then we have

$$\tan\frac{\psi}{2} = \frac{J_{f,af}S_{af}S_f}{J_{f,af}S_fS_{af} + 2Mab^3B}, \quad (61)$$

and the characteristic field B^* is given by

$$B^* \sim \frac{J_{f,af}S_{af}S_f}{Mab^3}. \quad (62)$$

In phase A, in a weak magnetic field, domains of the first type (with their magnetizations parallel to each other) are aligned with the field and the magnetization of the system is $M_{\max}/2$. The magnetizations of the FM layers in second-type domains (with their magnetizations antiparallel to each other in a zero magnetic field) behave in the same way as sublattice magnetizations in a bulk antiferromagnet; namely, they are directed almost at right angles to the external field.

As the field B increases, the angle ψ between the magnetizations decreases. The characteristic value B^* of the external magnetic field for which the angle ψ changes significantly can be found in the case of $R > R_c$ in the same way as that for phase B, and its order-of-magnitude estimate can be made using Eqs. (60) and (62). Therefore, the hysteresis loops for phases A and B differ only in the value of the magnetization in weak fields.

5.4. Experimental Data

There are many papers devoted to studying the relation between the interface roughness and the value of magnetoresistance. However, their discussion is beyond the scope of this review. We consider only the experimental data on the mutual orientation of the order parameters and on the domain structure. Such data have been obtained for the most part for Fe/Cr multilayer structures.

According to experimental neutron diffraction data [33, 34], Fe/Cr multilayers are ferromagnet–uncompensated-antiferromagnet structures. For thickness $a <$ 45 Å, chromium layers consist of ferromagnetic atomic planes with antiparallel orientation of spins in adjacent planes. The spins of chromium atoms lie in these planes, which, in turn, are parallel (on the average) to the interfaces between the layers. An analogous magnetic structure has also been observed in manganese layers in Fe/Mn multilayers [35, 36]. Therefore, the theory described above is applicable to Fe/Cr and Fe/Mn structures, and experiments on these structures can be performed to verify this theory.

In [37], domain structures in Fe/Cr multilayers were reported to be detected using polarized neutrons. However, the experimental data were not interpreted in [37] as those corresponding to the partition of a multilayer into regions with parallel and antiparallel mutual orientations of the magnetizations of adjacent FM layers. Instead, it was concluded that the magnetizations of adjacent layers are antiparallel to each other and that a multilayer breaks up into 180° domains running through the structure. The reason for the occurrence of this state, which is not favored energetically (because there is no gain in energy compensating for the energy that is required for the formation of a DW), was not discussed in [37].

In [38], an Fe/Cr multilayer was investigated in which the average thickness of AFM layers corresponded to the antiparallel mutual orientation of the magnetizations of adjacent FM layers. It was found that, as the roughness of the interfaces increases, the volume fraction of regions with parallel mutual orientation of the magnetizations of adjacent FM layers increases and can be as high as 50%.

6. CONCLUSIONS

(1) Due to the frustration caused by the roughness of the interfaces, DWs of a new type arise in magnetic multilayer structures.

(2) The thickness of these DWs is dictated by the balance of the exchange interactions in the interior of the layers and between them. The DW thickness in multilayers with a nonmagnetic spacer and in multilayers with an AFM spacer is smaller and much smaller, respectively, than the thickness of a conventional DW.

(3) The magnetic phase diagram and, therefore, the magnetic and galvanomagnetic characteristics of a

magnetic multilayer structure depend critically on the roughness of the interfaces between the layers.

It is desirable to perform complex studies, including the determination of the characteristics of the surface of layers during their deposition in a wide range of technological parameters, and to study the micromagnetic state of layers, magnetization curves, the dynamics of magnetization reversal, ferromagnetic resonance, and galvanomagnetic characteristics.

The determination of the relationship between the structure and properties of multilayers will make it possible to vary the technological parameters in such a way as to optimize the characteristics of magnetic multilayer structures for various practical applications.

ACKNOWLEDGMENTS

The authors are grateful to Ecole Centrale de Lille for providing conditions conducive to fruitful work.

This study was supported by CRDF and the Ministry of Education of the Russian Federation (grant no. VZ-010-0) and by PICS/RFBR (grant no. 1573/02-02-22002).

REFERENCES

1. M. N. Baibich, J. M. Broto, A. Fert, *et al.*, Phys. Rev. Lett. **61** (21), 2472 (1988).
2. Y. Yafet, Phys. Rev. B **36** (7), 3948 (1987).
3. P. Bruno and C. Chappert, Phys. Rev. B **46** (1), 261 (1992).
4. P. Bruno, Phys. Rev. B **52** (1), 411 (1995).
5. M. D. Stiles, Phys. Rev. B **48** (10), 7238 (1993).
6. L. Nordstrom, P. Lang, R. Zeller, and P. H. Dederichs, Phys. Rev. B **50** (17), 13058 (1994).
7. P. Bruno, J. Phys.: Condens. Matter **11** (48), 9403 (1999).
8. P. M. Levy and S. Zhang, J. Magn. Magn. Mater. **151** (3), 315 (1995).
9. R. Ribas and B. Dieny, Phys. Lett. A **167** (1), 103 (1992).
10. A. I. Morosov and A. S. Sigov, Pis'ma Zh. Éksp. Teor. Fiz. **61** (11), 893 (1995) [JETP Lett. **61**, 911 (1995)].
11. L. D. Landau and E. M. Lifshitz, *Course of Theoretical Physics*, Vol. 8: *Electrodynamics of Continuous Media*, 2nd ed. (Nauka, Moscow, 1982; Pergamon, Oxford, 1984).
12. A. I. Morosov and A. S. Sigov, Fiz. Tverd. Tela (St. Petersburg) **39** (7), 1244 (1997) [Phys. Solid State **39**, 1104 (1997)].
13. J. C. Slonczewski, Phys. Rev. Lett. **67** (22), 3172 (1991).
14. A. Dinia, S. Zoll, M. Gester, *et al.*, Eur. Phys. J. B **5** (1), 203 (1998).
15. C. H. Marrows, J. Hickey, M. Herrman, *et al.*, Phys. Rev. B **61** (6), 4131 (2000).
16. E. Bauer, T. Duden, H. Pinkvos, *et al.*, J. Magn. Magn. Mater. **156** (1), 1 (1996).
17. T. Zimmermann, J. Zweck, and H. Hoffmann, J. Magn. Magn. Mater. **149** (3), 409 (1995).
18. A. Kubetzka, M. Bode, O. Piezsch, and R. Wiesendanger, Phys. Rev. Lett. **88**, 057201 (2002).
19. V. D. Levchenko, A. I. Morosov, and A. S. Sigov, Pis'ma Zh. Éksp. Teor. Fiz. **71** (9), 544 (2000) [JETP Lett. **71**, 373 (2000)].
20. V. D. Levchenko, A. I. Morosov, A. S. Sigov, and Yu. S. Sigov, Zh. Éksp. Teor. Fiz. **114** (5), 1817 (1998) [JETP **87**, 985 (1998)].
21. V. D. Levchenko, A. I. Morosov, and A. S. Sigov, Zh. Éksp. Teor. Fiz. **121** (5), 1149 (2002) [JETP **94**, 985 (2002)].
22. A. Berger and H. Hopster, Phys. Rev. Lett. **73** (1), 193 (1994).
23. E. J. Escorcia-Aparicio, H. J. Choi, W. L. Ling, *et al.*, Phys. Rev. Lett. **81** (10), 2144 (1998).
24. J. C. Slonczewski, J. Magn. Magn. Mater. **150** (1), 13 (1995).
25. V. D. Levchenko, A. I. Morosov, and A. S. Sigov, Fiz. Tverd. Tela (St. Petersburg) **44** (1), 128 (2002) [Phys. Solid State **44**, 133 (2002)].
26. A. I. Morosov and A. S. Sigov, Fiz. Tverd. Tela (St. Petersburg) **44** (11), 2004 (2002) [Phys. Solid State **44**, 2098 (2002)].
27. A. P. Malozemoff, Phys. Rev. B **35** (7), 3679 (1987).
28. D. Mauri, H. C. Siegmann, P. S. Bagus, and E. Kag, J. Appl. Phys. **62** (7), 3047 (1987).
29. J. Nogues and I. K. Schuller, J. Magn. Magn. Mater. **192** (2), 203 (1999).
30. E. J. Escorcia-Aparicio, J. H. Wolfe, H. J. Choi, *et al.*, Phys. Rev. B **59** (18), 11892 (1999).
31. R. Arias and D. L. Mills, Phys. Rev. B **59** (18), 11871 (1999).
32. A. I. Morosov and A. S. Sigov, Fiz. Tverd. Tela (St. Petersburg) **41** (7), 1240 (1999) [Phys. Solid State **41**, 1130 (1999)].
33. A. Schreyer, C. F. Majkrzak, Th. Zeidler, *et al.*, Phys. Rev. Lett. **79** (24), 4914 (1997).
34. P. Bodeker, A. Schreyer, and H. Zabel, Phys. Rev. B **59** (14), 9408 (1999).
35. M. Chirita, G. Robins, R. L. Stamp, *et al.*, Phys. Rev. B **58** (2), 869 (1998).
36. S. Yan, R. Schreiber, F. Voges, *et al.*, Phys. Rev. B **59** (18), R11641 (1999).
37. D. L. Nagy, L. Bottyan, B. Croonenborghs, *et al.*, Phys. Rev. Lett. **88**, 157202 (2002).
38. A. Paul, J. Magn. Magn. Mater. **240** (1–3), 497 (2002).

Translated by Yu. Epifanov